Theor Chim Acta (1986) 69: 369-391

Theoretica Chimica Acta

Extended π-networks with multiple spin-pairing phases: resonance-theory calculations on poly-polyphenanthrenes*

G. E. Hite, A. Metropoulos, D. J. Klein, T. G. Schmalz and W. A. Seitz**

Theoretical Chemical Physics Group Department of Marine Sciences Texas A and M University at Galveston, Galveston, Texas 77553, USA

(Received August 26, 1985/Accepted January 6, 1986)

The poly-polyphenanthrene family of extended π-network strips with members ranging from polyacetylene to graphite is considered in terms of the locally correlated valence-bond or Heisenberg Hamiltonian. Resonance theory wavefunctions which provide a variational upper bound to the ground state energy are developed in a graph-theoretic formalism extendable to more general localized wavefunction cluster expansions. The graph-theoretic formalism facilitates the use of general transfer matrix techniques, which are especially powerful in application to quasi-one-dimensional systems such as are illustratively treated here. It is argued that these strips exhibit states of different long-range spin-pairing orderings. Novel properties associated with these different resulting phases are briefly indicated, including the possibilities of solitonic excitations and the reactivity at the ends of the strips. The qualitative arguments are supported by numerical calculations for strips up to width 8.

Key words: π-network polymers — Valence-bond model — Resonance theory — Long-range order — Bond localization — Solitonic excitations — Transfer matrices

1. Introduction

Because it includes electron correlation explicitly, the valence-bond model has played a fundamental role in understanding chemical bonding since its introduction in the early days of quantum chemistry [1]. In physics, the formally identical

* Research supported by The Robert A. Welch Foundation of Houston, Texas

** *Permanent address*: Theoretical Chemistry Institute, The National Hellenic Research Foundation, 48 Vassileos Konstantinou Avenue, Athens 501/1, Greece

Heisenberg spin Hamiltonian [2] has been widely applied in the study of the electronic properties of infinite many-body systems. While these models are readily solved for small finite systems [3] by explicit construction and diagonalization of the Hamiltonian matrix in a complete basis, they have not been exactly solved for infinite systems except for a few special cases (e.g., the ground-state energy for the homogeneous 1-dimensional linear chain is known) [4]. Particularly for two and three dimensional infinite lattices, various approximate calculations have been carried out, often with regard to the statistical mechanics of magnetic systems [5]. In this paper we introduce an approximate solution technique for the Heisenberg or valence bond model which produces a variational upper bound to the ground state energy of strips cut from an infinite 2-dimensional lattice such that the longitudinal dimension of the strip is infinite but the transverse dimension is small and finite. By extrapolating these finite width results we obtain an estimate of, and a bound for, the energy per site of the full 2-dimensional lattice.

In this paper we will consider systems of chemical interest; specifically, we consider strips cut from the 2-dimensional hexagonal (honeycomb) lattice. Each site of the lattice can be taken to represent an sp^2 carbon atom with one π-orbital perpendicular to the plane of the lattice and with one π-electron per site. Under this interpretation the infinite 2-dimensional lattice represents graphite while strips cut from the lattice represent conjugated benzenoid hydrocarbons of infinite length. Recent experimental work on linear π-electron polymers (e.g., polyacetylene) has yielded a number of unusual electronic properties including high conductivities. Though not yet fully characterized, some recently synthesized polymers have been argued to contain chains of benzenoid hydrocarbons which may be viewed as "strips" taken from the 2-dimensional hexagonal lattice [6]. Since finite benzenoid hydrocarbons are an especially stable class of organic molecules whose relative stabilities have been successfully studied via the valence-bond model, we expect that the valence-bond or Heisenberg model should be capable of meaningful predictions concerning the stability of π-electron polymers as well [7].

To facilitate the evaluation of matrix elements for the infinite-length strips we introduce a *transfer matrix* which effectively builds the contribution from a single "link" of the infinite strip into the matrix element. While the transfer matrix technique is a powerful general tool which has long been used in statistical mechanics [8, 9], and has recently been applied to several graph-theoretic enumeration problems [10], it has not yet been widely exploited in the context we describe here. In this paper we illustrate the technique by applying it to the series of strips of the *poly-polyphenanthrene* family. The $w = 2$ (polyphenanthrene) and $w = 3$ members of the family are shown in the lower two pictures in Fig. 1. The $w = 1$ limiting member of the family is cis-polyacetylene while the $w = \infty$ limiting member is graphite.

Section 2 of this paper introduces the Heisenberg model Hamiltonian and discusses its solution via graph-theoretical valence-bond methods. Sect. 3 generalizes the results of Sect. 2 to infinite-length systems. Sect. 4 describes the construction of the transfer matrix. Sect. 5 describes the evaluation of overlap and Hamiltonian

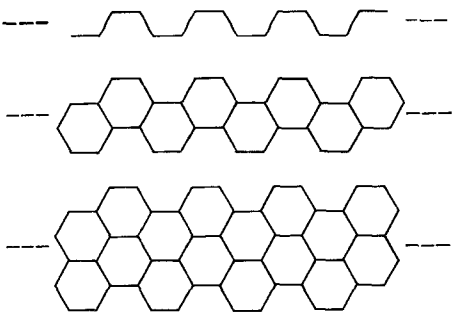

Fig. 1. The width $w = 1$, 2, and 3 strips: (cis)-polyacetylene, polyphenanthrene, and polyphenanthrephenanthrene

matrix elements. In Sect. 6 we show how these results simplify in the limit of infinite strip length. In Sect. 7 we present the numerical results for the poly-polyphenanthrene strips. Section 8 discusses some of the implications of these results.

2. Graph theoretic treatment of the Heisenberg (valence-bond) Hamiltonian

The Heisenberg Hamiltonian with nearest neighbor interactions only may be written as

$$H = \sum_{j \sim k} J_{jk}(2\boldsymbol{s}_j \cdot \boldsymbol{s}_k + \tfrac{1}{2}), \tag{2.1}$$

where j and k label sites, with $j \sim k$ indicating a nearest neighbor pair. The $\boldsymbol{s}_j$ are spin operators, and $2\boldsymbol{s}_j \cdot \boldsymbol{s}_k + \frac{1}{2}$ is the exchange operator. In this work we will assume that all sites and all bonds of the system are identical, so that all of the J_{jk} are equal to the same (positive) constant J. Often J is termed an "exchange integral" though it is in fact a more complicated sort of exchange parameter which can simply be chosen empirically [11]. Several authors have emphasized that the valence-bond Hamiltonian can be written in exactly the same form as Eq. (2.1) [12]. We will therefore make use of standard VB concepts [13] in analyzing the solution of (2.1).

It is well known that, for systems with a bipartite system graph Γ, a complete basis of covalent states can be generated by considering *Rumer diagrams*, wherein each point of the A (starred) subgraph is joined (spin paired) to one and only one point of the B (unstarred) subgraph. Not all Rumer diagrams are linearly independent, but a complete, linearly independent, basis can be generated by restricting attention to those Rumer diagrams in which no two joining lines cross. By way of illustration the independent Rumer diagrams for benzene are shown in Fig. 2a.

Matrix elements of the Heisenberg Hamiltonian between any two Rumer structures R and R' can be found by considering the *superposition diagram* obtained by superimposing the two Rumer diagrams. The superposition diagram partitions into different connected pieces, which for singlets are of just two types: *small*

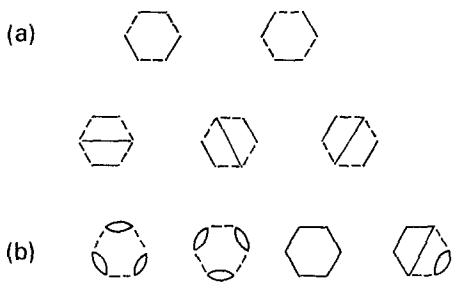

Fig. 2. (**a**) The independent Rumer structures for benzene. *Top line*: Kekulé structures. *Bottom line*: Dewar structures (**b**) Examples of superposition diagrams which can be generated from the Rumer diagrams of part (**a**)

islands consisting of two sites spin-paired in both ket and bra, and *big islands* consisting of an even number of four or more sites connected in a cycle. Figure 2b shows some of the superposition diagrams of benzene and the various islands associated with each. For one unnormalized choice of Rumer state basis, the overlap between two Rumer structures is given by Pauling's island counting formula [14],

$$\langle R|R'\rangle = \pm 2^{i+I}, \tag{2.2}$$

where i and I are the numbers of small and big islands in the superposition diagram for R and R'. Often the lines in the Rumer and superposition diagrams are directed, but this is redundant in the present case if the lines are always chosen to be directed from a starred to an unstarred site. Then the sign in (2.2) is always positive. The matrix elements of the products of spin operators appearing in the Hamiltonian are given in terms of these overlaps by

$$\langle R|\boldsymbol{s}_j \cdot \boldsymbol{s}_k|R'\rangle = \mp f\langle R|R'\rangle, \tag{2.3}$$

where the factor f is either 3/4 or 0, depending on whether j and k are in the same or different islands of the superposition diagram for R and R'. The sign in (2.3) is always negative (for nearest-neighbor pairs) with our choice of direction for lines in superposition diagrams.

For small systems (2.2) and (2.3) can be used to construct the full Hamiltonian matrix which can be diagonalized to yield the exact full singlet manifold. Unfortunately, the number of Rumer structures is an exponentially growing function of system size, so for larger systems basis truncation approximations are frequently employed.

Chemically, by far the most important basis functions are the *Kekulé structures*, i.e., those Rumer diagrams which contain only nearest-neighbor spin pairings (illustrated in the top line of Fig. 2a). Alternatively the Kekulé structures are the lowest energy structures and so should make stronger ground-state contributions. In the simple resonance theory *ansatz* [15, 16] which has been widely applied to benzenoid hydrocarbons, the (singlet) ground-state wavefunction of an aromatic system is expanded in terms of Kekulé structures only. Furthermore, the

Table 1. Comparison of exact and resonance theory Heisenberg energies for finite benzenoid hydrocarbons

L	Molecule	E^{Exact}/J [a]	E^{RT}/J [b]
1	Benzene	−8.606	−8.400
2	Naphthalene	−15.040	−14.364
3	Phenanthrene	−21.523	−20.514
4	Chrysene	−27.995	−26.577
5	Picene	−34.471	−32.679

[a] [3(a)]

[b] Calculated from the finite version of the transfer matrix method described in Sects. 4 and 5

wavefunction is often taken as the unweighted sum over all possible Kekulé structures

$$|\Psi\rangle = \sum_K |K\rangle, \tag{2.4}$$

which can be viewed as the leading term in a wavefunction cluster expansion. The associated resonance-theoretic energy expectation value is

$$E^{\text{RT}} = \frac{\langle\Psi|H|\Psi\rangle}{\langle\Psi|\Psi\rangle} \tag{2.5}$$

and yields an upper bound to the exact ground-state energy to the VB model for the system. In the remainder of the paper we will generally omit the superscript RT, but all equations should be understood to refer to resonance theory energy and wavefunction approximations.

In Table 1 we compare the energy calculated from (2.5) with the exact Heisenberg energy for a series of small benzenoid hydrocarbons. The resonance theory *ansatz* is seen roughly to reproduce the dependence of the exact ground-state energy on system size. Alternatively one can view the restriction to the space of Kekulé structures to define a new resonance theory model, the first-order contribution of which is just the representation of the Heisenberg (VB) model on this subspace. Then in lieu of higher-order contributions one could simply reparameterize the resonance theory model. Thence our resonance theory *ansatz* is a beginning toward the study of this (rather chemically appealing) resonance theory model. In the next section we will apply the resonance-theory wavefunction to infinite strips.

3. Resonance theory treatment of infinite strips

The graph theoretic methods in Sect. 2 can be carried over directly to infinite systems. The matrix elements in (2.4) are obtained as sums over superposition graphs $G \in S(\Gamma)$ where $S(\Gamma)$ is the set of all superposition graphs [17]. Now, the same G may generally arise from several different $\langle K|K'\rangle$. If the spin-pairings in any big island are interchanged between ket and bra, then the same G still

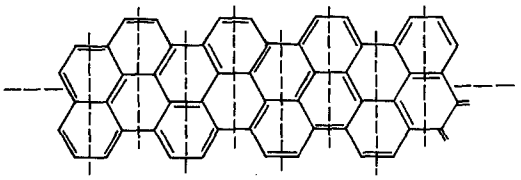

Fig. 3. A width $w=3$ strip with $Q=1$ double bonds at each column position, located by (transverse) *dotted lines*

occurs, and thus a given $G \in S(\Gamma)$ will arise $2^{I(G)}$ times where $I(G)$ is the number of big islands in G. Using this fact and (2.2) we obtain

$$\langle \psi | \psi \rangle = \sum_{G \in S(\Gamma)} 2^{i(G)} 4^{I(G)}. \tag{3.1}$$

A similar analysis of the Hamiltonian matrix element over $|\psi\rangle$ leads to

$$\langle \psi | H | \psi \rangle = -\tfrac{3}{2} J \sum_{G \in S(\Gamma)} N(G, \Gamma) 2^{i(G)} 4^{I(G)}, \tag{3.2}$$

where $N(G, \Gamma)$ is the number of bonds in Γ such that both ends of the bond are in the same island of G. In Sect. 4 we utilize the fact that the requisite matrix elements in (3.1), and also in (3.2), are graph-theoretic generating functions to develop a transfer matrix method to evaluate the infinite sums.

For systems with translational symmetry, a useful simplification occurs in that the Hamiltonian matrix is asymptotically block diagonal [7]. For the members of the sequence of graphs in Fig. 1, it can be seen that for a given Kekulé structure, the number, Q, of longitudinal bonds at any position along the strip must be the same. As an example consider Kekulé structures for a width $w=3$ strip. Two such Kekulé structures are shown in Figs. 3 and 4. There various (local) *positions* along the polymer strip are identified by transverse dotted lines. Note that for the Kekulé structure of Fig. 3, every position has exactly one longitudinal spin-pairing; moreover, no matter how the Kekulé structure is continued to either the right or the left, this statement remains true. Similar comments apply to the Kekulé structure of Fig. 4, where in this case there are exactly two longitudinal spin-pairings at every position. In fact, the number Q of longitudinal spin-pairings at any position for a Kekulé structure of width w is fixed down the entire length of the strip. (This may be proved as in section 5 of Ref. [18].) Kekulé structures with any (integer) value for Q from 0 to w are possible, and since the value of Q at one position implies the same value everywhere, the value of Q identifies a particular type of *long-range order.*

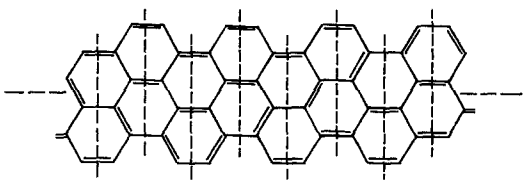

Fig. 4. A width $w=3$ strip with $Q=2$ double bonds at each position located by (transverse) *dotted lines*

Kekulé states with different Q values do not mix together in the limit of long strips. To see this, first note that, if $|K\rangle$ and $|K'\rangle$ are two *normalized* Kekulé states with Q and $Q' \neq Q$, then $|K\rangle$ and $|K'\rangle$ differ in every one of the (say L) positions along the whole length of the strip. Next note that the overlap $\langle K|K'\rangle$ is proportional to s^L where s is the overlap per position and $s<1$. Thus $\langle K|K'\rangle \to 0$ as $L \to \infty$, and likewise for the matrix element over any ordinary operator which effects a significant change at no more than a few positions. As a consequence the Hamiltonian (and overlap) matrix on the Kekulé basis is asymptotically block diagonal with regard to Q. Each block corresponds to a different long-range spin-pairing order as identified by the *resonance quantum number Q*.

Because Kekulé states of different Q do not mix, the resonance theory wavefunction (2.4) is restricted to

$$|\psi_Q\rangle = \sum_{K \sim Q} |K\rangle, \tag{3.3}$$

where the sum is restricted to all Kekulé structures with a given resonance quantum number Q, with the ground state being that Q which minimizes the energy

$$E_Q = \frac{\langle \psi_Q | H | \psi_Q \rangle}{\langle \psi_Q | \psi_Q \rangle}. \tag{3.4}$$

The restriction to Kekulé structures having a given Q will limit the sums in (3.1) and (3.2) to $G \in S_Q(\Gamma)$ where $S_Q(\Gamma)$ is the set of all superposition graphs associated with Q and embeddable in Γ.

4. Construction of the transfer matrix

A general approach for treating generating functions, such as those in (3.1) and (3.2), is the "transfer matrix" method often used in statistical mechanics [8, 9]. To develop this approach, consider an example superposition graph G with $Q=1$ on a width $w=2$ strip. Such an example is found in Fig. 5, where vertical dotted lines identify positions along the strip. To a given G we associate at each position a *local state* which is specified by: (a) a designation of which lattice links (of Γ) at the given position occur in G; and (b) a designation of which pairs of occupied lattice links are connected together by a sequence of G-bonds entirely to the left of the given position. The labels for the local states are also given in Fig. 5. Some details of the generation of local states for wider strips are described in Appendix A. We see that G determines the sequence of local states in each column along the whole length of the strip, and conversely the sequence of local states determines G. Thus a G-sum, as in (3.1) or (3.2), can be replaced by a sum over (a sequence of) local states. It is then desired to describe the transfer from one local state to the succeeding one(s) in a manner somehow "independent" of other local states elsewhere in the strip. Then G-sums over superposition diagrams can be written as multiple sums over (a finite set of) local states and the G-summand can be broken into a product of like terms.

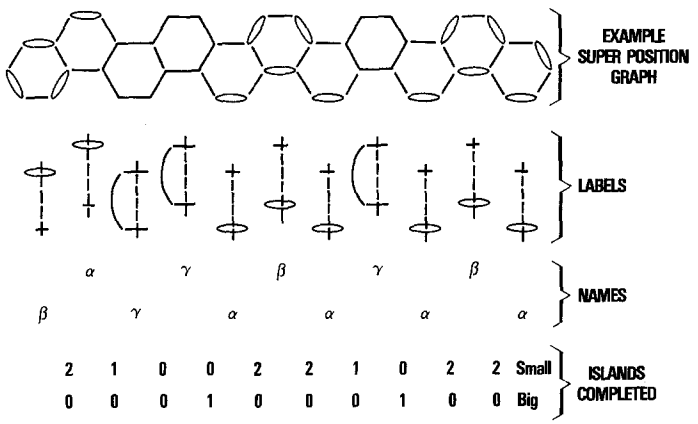

Fig. 5. An example $Q=1$ superposition graph on a width $w=2$ strip, and the graph's expression in terms of a sequence of local states, along with associated descriptors

The labelling of states is simplified by noting that a translation by one position followed by reflection (in a longitudinal plane normal to the plane of the strip) sends the strip into itself. This property is simply accounted for if local states related by this symmetry are given the same "name". For the superposition diagram ($w=2$, $Q=1$) shown in Fig. 5, the state labels refer to the states shown in Fig. 6. For the down positions the states are those of Fig. 6, while for the up positions the states are those of Fig. 6 reflected through a horizontal axis.

To develop the transfer matrix, note that only certain local states may immediately follow a given one. For our example case

$$\begin{aligned} &\alpha \to \alpha,\ \beta,\ \gamma \\ &\beta \to \alpha \\ &\gamma \to \alpha,\ \gamma. \end{aligned} \tag{4.1}$$

Further let $i(\zeta, \xi)$ and $I(\zeta, \xi)$ be the number of small and big islands completed in going from local state ξ to ζ at the succeeding position. Then we can define a *transfer matrix* $\boldsymbol{T}$ with columns labelled by local states and rows by possible succeeding local states

$$\boldsymbol{T}_{\zeta\xi} \equiv \begin{cases} 2^{i(\zeta,\xi)} 4^{I(\zeta,\xi)}; & \zeta \text{ can follow } \xi \\ 0; & \zeta \text{ cannot follow } \xi. \end{cases} \tag{4.2}$$

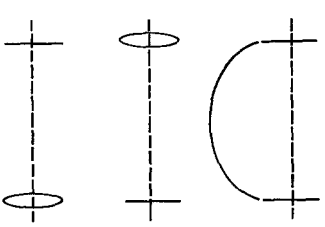

Fig. 6. The three possible local states for $Q=1$ and $w=2$

For the present example one may verify that

$$\boldsymbol{T}=\begin{pmatrix} 2^2 & 2^2 & 4^1 \\ 2^2 & 0 & 0 \\ 2^1 & 0 & 1 \end{pmatrix}, \tag{4.3}$$

where the basis is ordered as in (4.1). Now in the expression for $\langle\psi_Q|\psi_Q\rangle$ the multiple sum over local states is effected by matrix multiplication of the transfer matrix; moreover, the elements in (4.2) are defined so as to achieve the correct weights. Thus for a strip of length L we have

$$\langle\psi_Q|\psi_Q\rangle=(t|\boldsymbol{T}^L|i), \tag{4.4}$$

where $|i)$ and $|t)$, are respectively vectors for the initiating and terminating local states (at the left and right ends of the strip). The detailed form of these two vectors depends upon the particular nature of the strip ends. If cyclic boundary conditions are instituted, then the overlap would just be the trace of $\boldsymbol{T}^L$. Further details of the construction of the (generally non-Hermitian) transfer matrices are described in Appendix B.

5. Evaluation of overlap and Hamiltonian matrix elements

In our transfer matrix approach various superposition graphs are generated step by step (via repeated application of $\boldsymbol{T}$) starting from the left end of the strips. The same could be done starting from the right end, where the local states would be represented by designations interchanging left and right, i.e., the left-going local states for $w=2$ with $Q=1$ would appear like those of Figs. 5 or 6 viewed upside down. Then in place of (4.4) the overlap would be $(t'|\boldsymbol{T}^L|i')$, with $|i')$ and $|t')$ being respectively initiating, (terminating) states at the right, (left), end of the strip. An alternative, which proves more useful, e.g., on wider strips, involves propagating from both ends and joining left- and right-going local states somewhere on the strip, say between positions $n-1$ and n. The associated formula is

$$\langle\psi_Q|\psi_Q\rangle=(i'|\tilde{\boldsymbol{T}}^{L-n}\boldsymbol{C}\boldsymbol{T}^{n-1}|i), \tag{5.1}$$

where $\tilde{\boldsymbol{T}}$ is the transpose of $\boldsymbol{T}$ and $\boldsymbol{C}$ is a *connection matrix* effecting this joining. Here $\boldsymbol{C}_{\zeta\xi}$ is nonzero only if the left-going local states ξ can be successfully matched together with the right-going local state ζ; the nonzero value is a product of factors of 2, and 4, for each small, and big, island completed in the matching. In the $w=2$, $Q=1$ example

$$\boldsymbol{C}=\begin{pmatrix} 2^3 & 2^3 & 2\cdot 4 \\ 2^3 & 0 & 0 \\ 2\cdot 4 & 0 & 4 \end{pmatrix}, \tag{5.2}$$

where again the labellings for the rows and columns of $\boldsymbol{C}$ are ordered as in Fig. 6.

Next we turn to the evaluation of matrix elements of the Hamiltonian in (3.2). It is convenient to consider the contributions to the matrix element of the

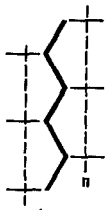

Fig. 7. An illustration for $w = 3$ of the $2w - 1 = 5$ diagonal bonds, of Eq. (5.3)

interaction $2\boldsymbol{s}_j \cdot \boldsymbol{s}_k$ separately for the diagonal bonds $j \sim k$ that are located between adjacent positions (see Fig. 7) and for the longitudinal bonds $j \sim k$ that are located at one position (see Fig. 8). For diagonal bonds from the argument leading to (4.5) one sees that the (unnormalized) expectation value of $2\boldsymbol{s}_j \cdot \boldsymbol{s}_k$ just modifies the elements of $\boldsymbol{C}$ involving the matching together of left- and right-going local states. That is, if ξ and ζ match together (at the position relevant for $j \sim k$) with j and k in the same island, then $\boldsymbol{C}_{\zeta\xi}$ is to be multiplied by $-\frac{3}{2}$; on the other hand, if j and k are in different islands $\boldsymbol{C}_{\zeta\xi}$ is to be replaced by zero. Thus for the (unnormalized) expectation value of the sum over all $2w-1$ diagonal-bond interactions between positions $n-1$ and n, we have

$$\langle \psi_Q | \sum_{j\sim k}^{n-1,n} 2\boldsymbol{s}_j \cdot \boldsymbol{s}_k | \psi_Q \rangle = -\tfrac{3}{2}(i' | \tilde{\boldsymbol{T}}^{L-n} \boldsymbol{V} \boldsymbol{T}^{n-1} | i), \tag{5.3}$$

where $\boldsymbol{V}_{\zeta\xi}$ is $\boldsymbol{C}_{\zeta\xi}$ times the number of links $j \sim k$ associated to position n such that both ends of the bond are in the same island of any one of the superposition diagrams associated to the pair ζ, ξ. For the $w = 2$, $Q = 1$ example

$$\boldsymbol{V} = \begin{pmatrix} 1 \cdot 2^3 & 1 \cdot 2^3 & 2 \cdot 2 \cdot 4 \\ 1 \cdot 2^3 & 0 & 0 \\ 2 \cdot 2 \cdot 4 & 0 & 3 \cdot 4^1 \end{pmatrix}. \tag{5.4}$$

Next matrix elements for the longitudinal bond interactions at position n, as indicated in Fig. 8 are to be evaluated. To achieve this, propagate superposition diagrams from the left and right ends up to positions $n-1$ and $n+1$, respectively. Then match the left- and right-going positions together (much as in the two preceding paragraphs) while counting the number of position-n longitudinal

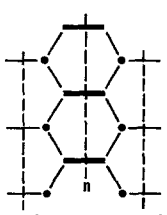

Fig. 8. An illustration for $w = 3$ of the w longitudinal bonds, Eq. (5.5)

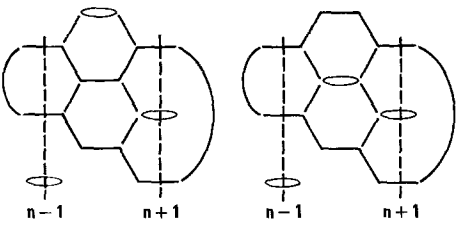

Fig. 9. An example showing two ways to join the same two (oppositely progressing) local states at positions $n-1$ and $n+1$

links with both ends in the same island. The associated formula entails a connection matrix $\boldsymbol{W}$,

$$\langle\psi_Q|\sum_{j\sim k}^{n} 2\boldsymbol{s}_j\cdot\boldsymbol{s}_k|\psi_Q\rangle=-\tfrac{3}{2}\,(i'|\tilde{\boldsymbol{T}}^{L-n-1}\boldsymbol{W}\boldsymbol{T}^{n-1}|i). \tag{5.5}$$

Here $\boldsymbol{W}_{\zeta\xi}$ is a sum over all the possible ways of matching ξ in column $n-1$ to ζ in column $n+1$. That there may be more than one way to effect a matching (for the present case) is illustrated in Fig. 9. (If there are no ways $\boldsymbol{W}_{\zeta\xi}$ is zero.) Each term in the sum is a product of two factors: the first factor is the number of position-n longitudinal (lattice) bonds with both ends in the same island; and the second factor involves 2, and 4, raised to the number of small, and big, islands completed in the associated particular way to make the matching between ξ and ζ. For the $w=2$, $Q=1$ example

$$\boldsymbol{W}=\begin{pmatrix} 1\cdot 2^5+1\cdot 2^5+2\cdot 2^2\cdot 4 & 1\cdot 2^5 & 1\cdot 2^3\cdot 4+2\cdot 2\cdot 4 \\ 1\cdot 2^5 & 1\cdot 2^3 & 4 \\ 2\cdot 2^2\cdot 4+2\cdot 2\cdot 4 & 1\cdot 2^3\cdot 4 & 1\cdot 2\cdot 4^2+2\cdot 2^0\cdot 4 \end{pmatrix}. \tag{5.6}$$

Further details of the construction of the (Hermitian) matrices $\boldsymbol{C}$, $\boldsymbol{V}$, $\boldsymbol{W}$ are discussed in Appendix C. The formulas of (5.1), (5.3), and (5.5) are the desired results from which we work.

6. Asymptotic infinite-strip behavior

The preceding formulas simplify in the limit of very long strips. The key point is that the maximum-magnitude eigenvalue of $\boldsymbol{T}$ dominates as the strip length $L\to\infty$. This can be seen if $\boldsymbol{T}$ is resolved in terms of its (generally non-adjoint) left and right eigenvectors, $(\mu, l|$ and $|\mu, r)$,

$$\boldsymbol{T}=\sum_{\mu}\mu|\mu, r)\,(\mu, l|, \tag{6.1}$$

where

$$(\mu, l|\mu', r)=\delta(\mu, \mu'). \tag{6.2}$$

Then substitution of (6.1) into (5.1) and retention of the leading asymptotic term yields

$$\langle\psi_Q|\psi_Q\rangle \to (i'|\lambda, l)\lambda^{L-n}(\lambda, r|\boldsymbol{C}|\lambda, r)\lambda^{n-1}(\lambda, l|i), \tag{6.3}$$

where it is supposed that there is a single maximum-magnitude eigenvalue λ. Similar treatments of (5.3) and (5.5) yield

$$\begin{aligned}\langle\psi_Q|\sum_{j\sim k}^{n,n-1} 2\boldsymbol{s}_j\cdot\boldsymbol{s}_k|\psi_Q\rangle &\to -\tfrac{3}{2}\lambda^{L-1}(i'|\lambda, l)(\lambda, r|\boldsymbol{V}|\lambda, r)(\lambda, l|i)\\ \langle\psi_Q|\sum_{j\sim k}^{n} 2\boldsymbol{s}_j\cdot\boldsymbol{s}_k|\psi_Q\rangle &\to -\tfrac{3}{2}\lambda^{L-2}(i'|\lambda, l)(\lambda, r|\boldsymbol{W}|\lambda, r)(\lambda, l|i)\end{aligned} \tag{6.4}$$

at least when position n is far from both ends of the strip. The ratios of the matrix elements of (6.4) to the overlap (6.3) give the expectation values for typical interactions, near position n. But as $L\to\infty$ there is an effective translational symmetry, so that L times the sum of these two expectation values gives the expectation value of H. Thus we have

$$\frac{\langle\psi_Q|H|\psi_Q\rangle}{L\langle\psi_Q|\psi_Q\rangle} \to -\tfrac{3}{2}J\frac{(\lambda, r|\{\boldsymbol{V}+\boldsymbol{W}/\lambda\}|\lambda, r)}{(\lambda, r|\boldsymbol{C}|\lambda, r)}, \tag{6.5}$$

which is the desired expression for the resonance theory energy per site for infinite strips in terms of the maximum eigenvalue and eigenvector of the transfer matrix and the three connection matrices $\boldsymbol{V}$, $\boldsymbol{W}$, and $\boldsymbol{C}$. It may be noted that (6.5) is explicitly independent of the strip ends, though we did make the implicit presumption that the ends are such that $(i'|\lambda, l)(\lambda, l|i)\neq 0$.

7. Numerical results

With the utilization of the transfer matrix technique resonance theory calculations on the VB model were carried out on a sequence of poly-polyphenanthrenes. Strips of widths $w=1$ to 8 with resonance quantum numbers $0\leq Q\leq w$ were treated. For each choice of Q for each of these w values, the *resonance energy* (per site), defined as the difference between the energy per site and the energy expectation value of a single Kekulé structure, is reported in Table 2 (except for the $Q=0$ and $Q=w$ cases which have resonance energies of zero). These results may be nicely organized if we plot (for each w) the resonance energies versus Q/w which ranges from 0 to 1 independently of w and thus may be taken as a local bond density for longitudinal bonds. At least for wide strips we expect the total resonance energy to depend on this bond density in a smooth way. Thus curves of resonance energy versus Q/w should approach a limiting ($w\to\infty$) curve, as indeed seems to occur. Figure 10 shows the $w=6$ and the extrapolated $w\to\infty$ curves. The higher curves (for $w=7$, 8) are close between these two curves.

Several things may be seen from these results. The Q value of the ground-state phase approaches $w/3$, thereby indicating that the π-bonds are equally distributed

Table 2

Strip width w	Resonance quantum number Q	Transfer matrix dimension $\#(w, Q)$	Resonance energy[a] $\Delta E/J$
2	1	3	−0.14745
3	1	6	−0.16564
	2	6	−0.10853
4	1	10	−0.15881
	2	20	−0.15300
	3	10	−0.08199
5	1	15	−0.14664
	2	50	−0.16940
	3	50	−0.12864
	4	15	−0.06533
6	1	21	−0.13415
	2	105	−0.17294
	3	165	−0.15445
	4	105	−0.10859
	5	21	−0.05417
7	1	28	−0.12269
	2	196	−0.17044
	3	490	−0.16784
	4	490	−0.13696
	5	196	−0.09326
	6	28	−0.04624
8	1	36	−0.11257
	2	336	−0.16512
	3	1176	−0.17379
	4	1766	−0.15509
	5	1176	−0.12145
	6	336	−0.08149
	7	36	−0.04033

[a] The energy per site of a single Kekulé reference structure is −0.75 J

over the three (equivalent) directions in graphite, as anticipated [18]. The extrapolated minimum resonance energy (at the graphite $w \to \infty$ limit) is −0.179 J and can be compared with the corresponding value of −0.15 J for benzene.

There appears to be a pattern of period 3 in w, as is also supported in the second paper following this one. The strips $w = 3m$ (for $m = 1, 2, 3, \ldots$) have a state ($Q = m$) very near the minimum (at $Q/w = 1/3$) of the resonance energy curves of Fig. 10, and as a consequence, this state is the nondegenerate overall ground state of especial stability (i.e., low energy). In Clar's nomenclature [19] these $w = 3m$ systems are "aromatic" or (for $m > 2$) perhaps slightly "superaromatic". The strips $w = 3m + 1$ (for $m = 0, 1, 2, \ldots$) have the $Q = m$ and $Q = m + 1$ states displaced respective distances of about $1/3w$ and $2/3w$ to the left and right of

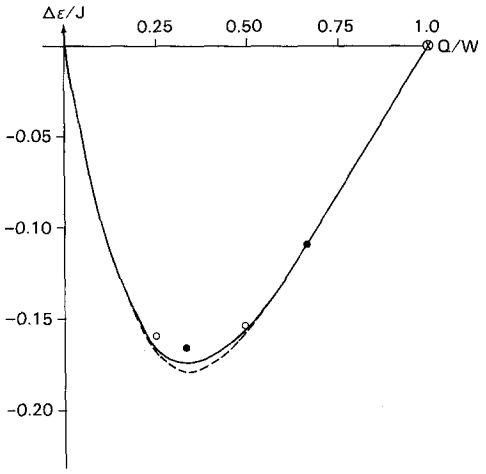

Fig. 10. Resonance energy per site versus Q/w for $w=6$ and the $w\to\infty$ extrapolated curve. The *solid* (and *open*) *dots* identify the two lowest near-degenerate (and nondegenerate) energies for $w=3$ (and $w=4$)

the $Q/w=\frac{1}{3}$ minimum in Fig. 10. Since the resonance energy curve is skewed with a gentler rise on the right, these two states are nearly degenerate, as verified for $m=1$ and 2 in Table 2 and as exactly true (by symmetry) for $m=0$. For smaller m these strips have a somewhat high energy and so are "subaromatic". Which of the two near degenerate states $Q=m$ or $Q=m+1$ is actually the ground-state is likely to be governed by higher-order wavefunction *ansätze*, as well as by higher-order interactions in the model and interactions with the environment. The third class of strips with $w=3m+2$ (for $m=0, 1, 2, \ldots$) is intermediate in features between the two already described; the $Q=m+1$ state is the nondegenerate ground state.

8. Discussion and conclusion

As we argued in Sect. 2, and based on many years of qualitative observations by organic chemists, resonance theory very often provides qualitative agreement with the observed physical and electronic properties of conjugated π-electron systems. In this section we will pursue several novel qualitative consequences of the locally-correlated resonance theory wave-function analysis for the family of π-electron polymers in Fig. 1. The novel features anticipated for this class of compounds may be viewed as a generalization of those already widely discussed for polyacetylene (the $w=1$ strip in Fig. 1); some of our discussion parallels earlier descriptions for polyacetylene [20]. Thus, while the synthesis and characterization of long-chain conjugated π-electron networks with a more complicated structure than polyacetylene (such as the poly-polyphenanthrene strips analyzed here) is currently a topic of considerable interest, we can anticipate theoretically a variety of novel electronic properties for these systems.

The block diagonalization of the Hamiltonian on the Kekulé basis into blocks labelled by the resonance quantum number Q implies that there is a discrete set

of long-range-spin-pairing order values possible, one for each block, with each identifying a different phase (in the thermodynamic sense). An immediate consequence of this picture of spin-pairing orderings concerns (partial) bond localization. The greater the frequency with which a given lattice link has a π-bond in the wavefunction for a phase Q (i.e., has the two associated π-electrons spin-paired together in the Kekulé structures of that phase), then the greater the bond order and the shorter the bond length for the lattice link. These lattice distortions in turn change the field in which the electrons move and so enhance their localization in bonds. At the extreme values of $Q = 0$ and $Q = w$ there occur just single Kekulé structures, so that bond localization occurs to the maximum extent.

There are several qualitative features that may be associated with our identification of various resonance phases. One aspect concerns the role and nature of the (left and right) ends of the polymer strips. First, if one draws a Kekulé structure on a finite strip, then a unique value of Q, say Q_0, seems to arise; that is, the nature of the strip ends seems to determine Q for the drawing. This is illustrated in Figs. 3 and 4 if the pictures there are supposed to exhibit the whole finite strip. In particular if the ends are cut off "straight", such as in Fig. 3, then it may be seen that in a (global) Kekulé structure $Q = 1$, regardless of strip width w. Now if the energy per "position" is lower for a quantum number $Q_<$ different than Q_0 obtained by drawing in a global Kekulé structure, then the overall ground state for a sufficiently long strip should in the bulk still look like the $Q_<$-phase. This can be accomplished by introducing a few "non-bonded" electrons (or other defects) near the ends of the strip, as illustrated in Fig. 11. Of course such a structure with $Q = Q_<$ is only like a Kekulé state in the bulk of the strip, away from the ends. In such a case the ends with non-bonding electrons (or other defects) should be especially reactive. Thus one can anticipate that in an actual polymerization process the ends will tend to become accommodated to the preferred lowest energy Q value.

These considerations [21] concerning the ends have some computational implications as well. Generally a method should not be restricted to focus only on global Kekulé structures dependent on particular strip ends. For if it were so restricted, instead of yielding the correct ground state, the method would identify the lowest-lying state of the Q-block "dictated" by the strip ends. One might imagine

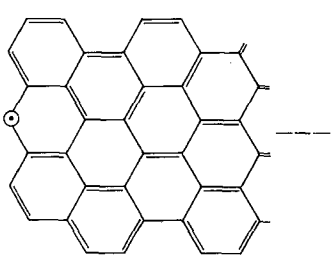

Fig. 11. The "left" end of a $w = 4$ strip, with $Q = 2$ and a non-bonded (unpaired) electron encircled at the left

that such (often overlooked) effects can be of importance for larger peri-condensed species of a dozen or more rings. For the poly-polyphenanthrene strips the problem could be by-passed by using cylic boundary conditions.

Another aspect associated with the various resonance phases concerns the possibility of solitonic excited states. If a non-bonding π-electron is introduced (away from the strip ends), then different phases must occur to the left and right of this singular electron. Moreover, the difference in Q values for the two phases (which this singularity separates) is either $\Delta Q = +1$ or $\Delta Q = -1$, depending on whether the unpaired electron occurs on a "starred" or "unstarred" site. This circumstance is illustrated in Fig. 12. Now such a state would not readily decay directly to a lower-lying state such as that associated to either the left or right phase, because all these states differ in many positions, when the unpaired electron is well away from the ends of the strip. The unpaired electron could "hop" a short distance and so ultimately travel along the strip. Hence it seems that such an excited state should be *long-lived* and (perhaps) also nondispersive. Thus it has two *solitonic* features [20]. The final feature of solitons, the noninteraction of two impinging solitons, should also occur, unless they happen to annihilate to give photon(s) and/or phonon(s). If instead of an unpaired electron, a π-electron vacancy or additional π-electron is placed at the defect site, a charged solitonic excitation occurs. It is seen that the neutral excitation has charge and spin, $q = 0$ and $s = \frac{1}{2}$, while the charged excitations have $q = \pm 1$ and $s = 0$. This parallels earlier descriptions [20] of excitations in polyacetylene, though the various conclusions there are usually justified in terms of the Hückel model.

Qualitatively rather different behavior [22] is anticipated depending on whether the lowest energy phases are degenerate or not. If degenerate, then individual single-site solitons should be observable. If the phases are very nearly degenerate (but not exactly so, as in $w = 3m + 1$ strips) then modifications of the environment (e.g., pH) could induce the passage of a soliton to effect the change from one phase to the other; this might then act as a molecular switching device to monitor the environment [23]. If the lowest energy phase is non-degenerate, then a $\Delta Q = +1$ soliton and $\Delta Q = -1$ *antisoliton* will attract one another, so that the amount of high-energy phase between them is limited. In this case even if the soliton and antisoliton are of like charge, *confinement* occurs, i.e., the attraction due to the intervening high-energy phase dominates (strongly) over Coulomb repulsion at sufficiently long range. Thus for $w = 3m$ and $w = 3m + 2$ only "bisolitonic" states should be relevant. An additional feature for the present strips is that a number ($\doteq w$) of soliton (and antisoliton) states should arise depending on how the singular electron is spread out transversely, across the strip.

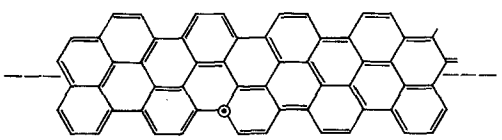

Fig. 12. An encircled unpaired electron separating $Q = 1$ and $Q = 2$ phases on the *left* and *right*

Finally there is the question of whether the present ideas persist when the restriction to Kekulé structures is not made. Beyond Kekulé structures the next higher energy Rumer-basis structures that mix most strongly with the Kekulé structures are those with a long-bond (or spin-pairing) between sites which are not too distant but are non-nearest neighbors. Such a long-bond (as for instance in the Dewar structures of benzene in Fig. 2a) may be viewed as a nearby soliton-antisoliton pair (since every bond must connect a starred and unstarred site) and the admixture into the ground state may be viewed as a *vacuum fluctuation.* That such a long-bond consists of a (bound) soliton-antisoliton pair implies that the net change in Q across the long-bond as a whole is zero. That is, the long-range order can be preserved, although to a diminished extent. Indeed these ideas are already implicitly illustrated in quantitative calculations [24] for the VB model of polyacetylene. Moreover, it is of interest to note that if the next higher-order corrections to the nearest-neighbor VB model are considered, then the Kekulé structure picture tends to improve [25].

In summary, we have illustrated the application of a transfer matrix technique for evaluating expectation values for quasi-one-dimensional systems described by locally correlated wavefunctions. The technique was illustrated for resonance-theory wavefunctions, but could, for instance, also be applied to a wavefunction with independent localized pair excitations above an SCF determinant of localized orbitals.

Novel features of the resonance theory wavefunctions for poly-polyphenanthrenes have been discussed. The possibility of a resonance quantum number labelling different phases is a key focus of interest. Though quantitative results for excited states remain for future calculation, several qualitative features were considered - particularly in terms of solitons. It was argued that poly-polyphenanthrene strips fall into three distinct groups depending on whether the width $w=3m$, $w=3m+1$, or $w=3m+2$ ($m=0, 1, 2, \ldots$). Qualitative aspects of reactivity at the ends of strips of poly-polyphenanthrene were also indicated. Thus it seems that our view and the computational technique presented could be of general utility in studying extended polymer systems.

Appendix A. Characterization of local states

A general characterization of the local states for any strip width w and resonance quantum number Q, is needed to represent and generate them on a computer. We chose to represent each *local state* by a w-component vector, say σ, with the ith component σ_i taking (integer) values detailing the situation at the ith horizontal lattice bond in the local state being labelled. There are three general situations: first $\sigma_i=0$ if this ith lattice link is not occupied by a spin-pairing; second $\sigma_i=i$ if this ith link is occupied by two spin-pairings (constituting a small island); and third $\sigma_i=j\neq i$ if this ith link is occupied by a single spin-pairing (in a big island) with a path of spin-pairings entirely to the left of the current position connecting the spin-pairing at link i to one at link j. Finally, we number the lattice links from the innermost strip edge across the strip. Then for the $w=2$, $Q=1$ example

of Fig. 6, the three local states are represented as

$$\binom{0}{2}, \binom{1}{0}, \binom{2}{1} \tag{A1}$$

(where the innermost strip edge is considered to be at the top).

It is also useful to make an incomplete representation of local states, thereby partitioning them into different *classes*. This class label is simply a vector $\boldsymbol{u}$ with the i component giving the number (0, 1, or 2) of spin-pairings occupying the ith link in a local state. In the case of Eq. (A1) the class labels uniquely specify the local states, though this is (for $w \geq 4$) generally not true. For instance the two local states of Fig. 13 have the same class label, namely $\boldsymbol{u}$ with

$$u_1 = u_2 = u_3 = u_4 = 1. \tag{A2}$$

In fact the number of local states in a particular occupancy class is determined by the number of allowed ways of pairing up the "singly-occupied" links. In the picture labels, as in Fig. 5, this must be done without any of the connecting loops (on the left) crossing one another (since on our strips confined to two dimensions this would entail the unallowed situation of four spin-pairings incident at the same crossing site). Now the number of allowed ways of connecting a fixed (even-numbered) set of (singly-occupied) links is a well-known geometric problem which is also encountered [13, 15, 26] with Rumer basis states for pairing the same (even) number of different orbitals to an overall singlet. Thus if there are $2p$ singly-occupied positions in a class there are

$$\frac{(2p)!}{(p+1)!p!} \equiv n_p \tag{A3}$$

corresponding local states. The local states may be thought of as specified by a pair of labels: the first being the class label and the second being the "pairing path pattern" indicating which pairs of singly-occupied positions are "coupled together". This latter label may be viewed as a picture like a Rumer diagram (or a sequence of numbers like a Yamanouchi symbol).

We generated local states first constructing class labels and then the various Rumer-type diagrams associated with each class. The class labels for a given w and Q are just the different ways of choosing w numbers to be 0, 1, or 2 such

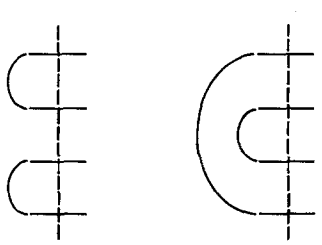

Fig. 13. Two local states (on a $Q = 2$, $w = 4$ strip) being in the same occupancy class

that their sum is $2Q$. Letting $2p$ and d be the number of singly- and doubly-occupied lattice links in a class label, it is seen that $p+d=Q$. The number of classes with a given w, p and d is a trinomial coefficient

$$\frac{w!}{(2p)!\,d!\,(w-2p-d)!}=\frac{w!}{(2p)!\,(Q-p)!\,(w-p-Q)!} \tag{A4}$$

and recalling (A.3), we see that the number of local states is

$$\#(w, Q)=\sum_p \frac{w!}{(Q-p)!\,(w-p-Q)!\,(p+1)!\,p!}. \tag{A5}$$

These numbers give the dimension of the space on which the transfer matrix is to act. Values for these numbers for $1\leq Q\leq w-1$ and $2\leq w\leq 8$ are given in Table 2 (also $\#(w, 0)=\#(w, w)=1$). It is seen that the handling of vectors on these corresponding spaces is feasable on current minicomputers for strips up through width $w\tilde{=}8$.

Appendix B. Treatment of the transfer matrix

In the determination of the transfer matrix it is convenient to consider whether two classes connect. We will consider the values of matrix elements between local states in classes u and v. These lattice-link occupancies on two adjacent columns are indicated (for $w=3$) in Fig. 14 where we also introduce (temporary) labels a_i and b_j for the occupancies of the intermediate diagonal lattice links. Since each site of the lattice is to be spin-paired in both bra and ket, the sum of the occupancies for the lattice links incident on any site should be 2. Thus

$$\begin{aligned}
&v_w && && +a_1 &&=2\\
&u_1 &&+a_1 &&+b_1 &&=2\\
&v_{w-1} &&+b_1 &&+a_2 &&=2\\
&u_2 &&+a_2 &&+b_2 &&=2\\
&&&&&\vdots\\
&v_1 &&+b_{w-1} &&+a_w &&=2\\
&u_w &&+a_w &&&&=2
\end{aligned} \tag{B1}$$

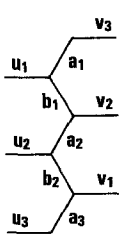

Fig. 14. An illustration of the identification between lattice links and occupancy labels

as is readily seen from Fig. 14. Now given u and v this set of equations may be solved progressively (from top to bottom) for the a_i and b_j. If at any step any one of these equations cannot be satisfied with a_i and b_j taking allowed occupancy values 0, 1, or 2, then there are no transfer matrix elements between local states of the classes u and v; that is, all these transfer matrix elements are zero. If an allowed solution to (B1) is found, then one has an evidently unique connection between these two classes; each local state (on the left) in class u is connected to a unique local state (on the right) in class v.

Since the larger transfer matrices turn out to be quite sparse, only (the locations and values of) the nonzero elements need be stored. The (right) eigenvector for the maximum modulus eigenvalue was found to be easily computed via the power method where one simply repeatedly applies $\boldsymbol{T}$ to a vector. Since the Frobenius-Perron theorem [27] applies to our current situation, the eigenvector sought has all its components of the same phase (which is conveniently chosen to be positive); hence a suitable initiating vector for the iterative eigenvalue-eigenvector routines is the vector with all components equal.

Appendix C. The connection matrices

For the method of computation of $\boldsymbol{C}_{\zeta\xi}$ consider the pattern ξ, ζ. Through the use of relations as in (B1) it is determined whether ξ and ζ may be adjoined, and if so, intervening occupied diagonal lattice links (in big islands or small islands) are located (by nonzero a_i and b_j). The small islands and their number thence are readily identified. Then one searches through ξ for a (big) island edge, i.e, $\xi_i = j \neq i$. Once such an edge is located it is "traced" through the ξ, a, b, ζ pattern: one passes from link i, to link $j = \xi_i$, then to the associated a component, etc. until finally returning to the initiating link i. Each traversed lattice link is "removed" so that the big island is purged from the pattern. This search continues deleting (and counting) each big island encountered. After so purging each big island with links in ξ, the search is continued through any remaining portion of ζ. Then the desired matrix element is

$$\boldsymbol{C}_{\zeta\xi} = 2^{i_c(\zeta,\xi)} 4^{I_c(\zeta,\xi)}, \tag{C1}$$

where $i_c(\zeta, \xi)$ and $I_c(\zeta, \xi)$ are the numbers of small and big islands counted in the ξ, ζ pattern.

The matrix element $\boldsymbol{V}_{\zeta\xi}$ is conveniently computed at the same time as $\boldsymbol{C}_{\zeta\xi}$, since $\boldsymbol{V}_{\zeta\xi}$ is just $\boldsymbol{C}_{\zeta\xi}$ times the number $N_d(\zeta, \xi)$ of diagonal lattice links with end-points in the same island of the ξ, ζ pattern. Contributions to $N_d(\zeta, \xi)$ come from small as well as large islands. The contribution from small islands is simply the number of doubly occupied diagonal lattice links, i.e., the number of times that $a_i = 2$ ($i = 1$ to w) and that $b_j = 2$ ($j = 1$ to $w-1$). For large islands the situation is more complicated, since not only must singly occupied diagonal lattice links be counted but also the unoccupied diagonal lattice links whose ends are in the same island, as illustrated by the example in Fig. 15. The contribution of this type can be

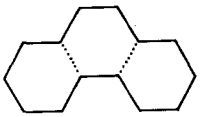

Fig. 15. A big island on a $w=2$ strip, with the two unoccupied diagonal links indicated by dotted lines having end-points in the same island

found by analysis of each individual big island "traced" out in the construction of $\boldsymbol{C}_{\zeta\xi}$.

To calculate the contribution from nearest-neighbor interactions of longitudinal lattice links, it is necessary to know when sites on the ends of a longitudinal link are in the same island. For $w \geq 3$ it is possible to have the situation where sites are in the same (large) island but for which the island's edge does not run along the link. This is illustrated in Fig. 16 To identify such cases it is necessary to know the occupancies of the diagonal links to the right and to the left of the position, say n, being considered. This is available if the local state at the $(n+1)^{\text{th}}$ position, ζ, and the $(n-1)^{\text{th}}$ position, ξ, are specified. If $\boldsymbol{W}_{\zeta\xi}$ designates the contribution of longitudinal lattice links for all possible intermediate local states ζ at the nth position, then $\boldsymbol{W}_{\zeta\xi}$ requires the consideration of patterns (ξ, η, ζ) spread out over three positions along the strip (rather than just two as for $\boldsymbol{C}$ or $\boldsymbol{V}$). In fact

$$\boldsymbol{W}_{\zeta\xi} = \sum_{\eta} \tilde{\boldsymbol{T}}_{\zeta\eta} \boldsymbol{C}_{\eta\xi} N_l(\zeta, \eta, \xi), \tag{C2}$$

where $N_l(\zeta, \eta, \xi)$ is the number of nearest-neighbor sites on longitudinal lattice links at position n such that the two sites of a pair are in the same island of the ξ, η, ζ pattern.

The number $N_l(\zeta, \eta, \xi)$ (just as $N_d(\zeta, \xi)$) has contributions from small as well as large islands. The contribution from small islands is simply the number of doubly occupied longitudinal lattice links, i.e., the number of times that $\eta_i = i$. For large islands the situation is more complicated, since not only must singly occupied longitudinal lattice links be counted, but also the unoccupied longitudinal lattice links whose ends are in the same island as illustrated by the example in Fig. 16. The latter contributions can be found by "tracing" each individual big island in the ξ, η, ζ pattern having longitudinal bonding in η.

In (C2) propagation from position $n+1$ to n (with $\boldsymbol{T}$) is envisioned followed by connection (with $\boldsymbol{C}$) between positions $n-1$ and n, with $\boldsymbol{T}_{\zeta\eta} \cdot \boldsymbol{C}_{\eta\xi}$ giving the appropriate weight factor for completion of big and small islands. But propagation

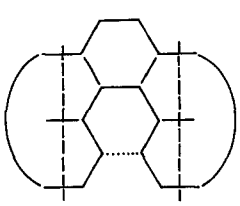

Fig. 16. A big island on a $w=3$ strip, with the unoccupied longitudinal link indicated by a *dotted line* having end-points in the same island

from position $n-1$ to n (with $\boldsymbol{T}$) followed by connection (with $\boldsymbol{C}$) between positions n and $n+1$ may also be envisioned. Thus

$$\sum_{\eta} \tilde{\boldsymbol{T}}_{\zeta\eta}\boldsymbol{C}_{\eta\xi} = \sum_{\eta} \boldsymbol{C}_{\zeta\eta} \cdot \boldsymbol{T}_{\eta\xi} \equiv \bar{\boldsymbol{C}}_{\zeta\xi}. \tag{C3}$$

This then can provide a partial check on the $\boldsymbol{C}$ and $\boldsymbol{T}$ matrices, used to construct $\boldsymbol{W}$, and $\boldsymbol{V}$.

Finally we note that the various connection matrices need not be stored, which is especially useful for $\boldsymbol{W}$ since it is relatively dense. That there is no need for storage occurs because only the matrix elements over $|\lambda, r)$ are required. Then, for instance, as each element of $\boldsymbol{W}_{\zeta\xi}$ is generated only its contribution $(\lambda, r|\zeta)\boldsymbol{W}_{\zeta\xi}(\xi|\lambda, r)$ to $(\lambda, r|\boldsymbol{W}|\lambda, r)$ is added to a continuously up-dated sum, which ultimately becomes the desired matrix element. As mentioned after (C2) the product $\tilde{\boldsymbol{T}}_{\zeta\eta}\boldsymbol{C}_{\eta\xi}$ is just the appropriate weight factor due to the number of big and the number of small islands completed in the pattern ξ, η, ζ. Since these numbers can easily be obtained at the same time $N_l(\zeta, \eta, \xi)$ is calculated, there is no need to form the product $\tilde{\boldsymbol{T}}_{\zeta\eta}\boldsymbol{C}_{\eta\xi}$ and consequently no need to store $\boldsymbol{C}$. If the matrix elements over $|\lambda, r)$ of $\bar{\boldsymbol{C}}$ are calculated, then (C3) requires that

$$(\lambda, r|\bar{\boldsymbol{C}}|\lambda, r) = \lambda(\lambda, r|\boldsymbol{C}|\lambda, r) \tag{C4}$$

and thus provides a more limited check than (C3) on the calculation.

References

1. Pauling L (1940) The nature of the chemical bond. Cornell University Press, Ithaca, New York
2. Van Vleck JH (1932) The theory of electric and magnetic susceptibilities. University Press, Oxford
3. Numerically exact computations for the ground state of the VB model have been performed for systems having up to 24 sites: (a) Alexander SA, Schmalz TG, J Am Chem Soc (submitted); (b) see also, Ramasesha S, Soos ZG (1984) Int J Quantum Chem 25:1003
4. The special case of the ground state of a cyclic chain without bond-alternation turns out to be exactly soluble by a complex many-body technique which has not been extended to other structures: Hulthen L (1938) Ark Mat Astron Fys A26:1
5. See, for example, Mattis DC (1965) The theory of magnetism. Harper and Row, New York
6. (a) Murakami M, Yoshimura S (1984) J Chem Soc Chem Commun p. 1649; (1985) Mol Cryst Liq Cryst 118:95; (b) Tanaka K, Ohzeki K, Yamabe T, Yata S (1984) Synth Met 9:41
7. (a) Seitz WA, Klein DJ, Schmalz TG, Graciá-Bach MA (1985) Chem Phys Lett 115:139; (b) Klein DJ, Schmalz TG, Hite GE, Metropoulos A, Seitz WA (1985) Chem Phys Lett 120:367
8. See, e.g., Thompson CJ (1972) Mathematical statistical mechanics. Macmillan Co, New York
9. Early references include: (a) Montroll EW (1941) J Chem Phys 9:706; (b) Kramers HA, Wannier GH (1941) Phys Rev 60:252; (c) Lassertre EN, Howe JP (1941) J Chem Phys 9:747; (d) Kubo R (1943) Busserion Kenkyu 1
10. For other graph-theoretic applications see, e.g., (a) Klein DJ (1980) J Stat Phys 23:561; (b) Derrida B (1981) J Phys A14 L5; (c) Derrida B, DeSeze L (1982) J Phys 43;475
11. There is also the question of a "proper" derivation of such models. See, e.g., (a) Van Vleck JH (1963) Phys Rev 49:232; (b) Simpson WT (1956) J Chem Phys 25:1124; (c) Herring C In: Rado GT, Stuhl H (ed) Magnetism 2B, Academic Press, NY, p. 1; (d) Buleavski LN (1966) Zh Eksp Teor Fiz 51:230; (e) Klein DJ, Foyt DC (1973) Phys. Rev 8A:2280; (f) White CT, Economou EN (1982) Phys Rev 18B:3959; (g) Malrieu JP, Maynau D (1982) J Am Chem Soc 104:3021 and 3029; (h) Poshusta RD, Klein DJ (1982) Phys Rev Lett 48:1555

12. See, e.g., (a) Van Vleck JH, Sherman A (1935) Rev Mod Phys 7:167; (b) Simpson WT (1962) Theories of electrons in molecules. Prentice-Hall, Englewood Cliffs, New Jersey
13. (a) See, e.g., Eyring H, Walter J, Kimball GE (1944) Quantum Chemistry, Chap. 13, John Wiley and Sons, New York; (b) Simpson WT (1962) Theories of electrons in molecules. Prentice-Hall, Englewood Cliffs, New Jersey
14. Pauling L (1933) J Chem Phys 1:280
15. Pauling L, Wheland GW (1933) J Chem Phys 1:362; (b) Pauling L, Sherman J (1933) J Chem Phys 1:679
16. (a) McGlynn SP, VanQuickenborne LG, Kinoshita M, Carroll DG (1972) Introduction to applied quantum chemistry, Section 6.2. Holt, Rinehart, and Winston, Inc, New York; (b) Herndon WC (1973) J Am Chem Soc 95:2404; (c) Herndon WC, Ellzey ML Jr (1974) J Am Chem Soc 96:6631
17. Such superposition graphs constructed only from Kekulé structures often arise in graph theory and are also termed Sachs graphs, as in Trinajstic N (1983) Chemical graph theory, vol II. CRC Press, Boca Raton, Florida
18. Klein DJ (1979) Int J Quantum Chem 138:293
19. Clar E (1972) The aromatic sextet. John Wiley and Sons, New York
20. (a) Su WP, Schrieffer JR, Heeger AJ (1979) Phys Rev Lett 42:1698; (b) Rice MJ (1979) Phys Lett 71A:152; (c) Su WP, Schrieffer JR, Heeger AJ (1980) Phys Rev B22:2099
21. The effects described here are in fact evident in earlier enumerations restricted to global Kekulé structures on a rather wide class of polyphene structures. See, e.g. (a) Yen TF (1971) Theor Chim Acta 20:399; (b) Stein SE, Brown RL (1985) Carbon 23:105
22. See, e.g., the reviews: (a) Heeger AJ (1981) Comments Solid State Phys 10:53; (b) Chien JCW (1981) J Pol Sci Lett 19:249; (c) Baughman RH, Bredas JL, Chance RR, Elsenbaumer RL, Shacklette LW (1982) Chem Rev 82:209; (d) Duke CB, Paton A, Salaneck WR (1982) Mol Cryst Liq Cryst 83:177
23. Carter FL (1984) Physica 10D:175
24. Klein DJ, Garcia-Bach MA (1979) Phys Rev 19B:877
25. Klein DJ (1982) J Phys 15A:661
26. Rumer G (1932) Nachr Ges Wiss Göttingen 1932:337
27. See, e.g., Gantmacher FR (1959) The theory of matrices, vol II, chap. 13. Chelsea, New York